

Induction Motor Bearing Fault Detection under Transient Conditions

Mustafa M. Ibrahim^a, Habeeb J. Nekad^{a*}

^aElectrical Engineering Department- College of Engineering, University of Basrah, Basrah-Iraq

Accepted 10 September 2013, Available online 01 October 2013, Vol.3, No.4 (October 2013)

Abstract

This paper introduces a method for diagnosis of bearing fault of induction motor under transient conditions. The q-axis component of the stator current signal is decomposed by using the discrete wavelet transform (DWT). The fault detection method is developed by using the artificial neural network (ANN) to identify the motor state. A dynamic model of the squirrel-cage induction motor taking account the bearing faults is developed using simulink/matlab. Simulation results show that the better performance of the proposed method.

Keywords: Induction motor, bearing fault, MCSA, DWT, ANN

1. Introduction

Due to the close relationship between motor system development and bearing assembly performance, it is difficult to imagine the progress of modern rotating machinery without consideration of the wide application of bearings. In addition, the faults arising in motors are often linked with bearing faults. In many instances, the accuracy of the instruments and devices used to monitor and control the motor system is highly dependent on the dynamic performance of bearings (W. Saadaui *et al*,2011).

Traditionally, diagnostics of bearings is carried out by means of monitoring of vibrations either of the bearings or the motor case. This method requires the use of accelerometers or other vibration sensors and appropriate devices for signal conditioning and can be expensive and not always simple to be performed. On the contrary, monitoring of stator current requires the use of a current probe that can also be employed for the diagnosis of faults (L. Frosini *et al*,2010).

Signal processing methods such as fast Fourier transform (FFT) are used to analysis the motor current signal in steady state conditions. The analysis of a non-stationary signal using the FFT does not give satisfactory results. Better results can be obtained using wavelet analysis. The advantages of using wavelet techniques for fault monitoring and diagnosis of induction motors is increasing because these techniques allow us to perform stator current signal analysis during transients. The wavelet technique can be used for a localized analysis in the time-frequency or time-scale domain. It is then a powerful tool for condition monitoring and fault diagnosis (M. E. Benbouzid *et al*,2000).

In this paper, an effective method is presented to bearing fault detection based on the MCSA method. Wavelet transform can be used to detect the fault under transient conditions. The q-axis component of the stator current signal is decomposed by using DWT. The fault detection method is implemented by means of an ANN that is trained using the RMS values of the wavelet coefficients.

2. Bearing Fault Signature

Bearing consists of two rings called the inner and outer rings. A set of balls or rolling elements placed in raceways rotate inside these rings as shown in Fig. (1). Bearing defects can occur as a result of fatigue of their material under normal operational conditions. First, cracks will appear on the tracks and on the balls. Then pitting and scuffing of material can quickly accelerate the wear of a bearing and intensive vibrations are generated as a result of the repetitive impacts of the moving components on the defect. For instance, when a rolling element contacts a defect on the inner or outer raceway, it produces an impact which in turn excites the structural modes of the bearing and its support (W. Saadaui *et al*,2011).

Bearing faults can be categorized into distributed and localized defects. Distributed defects affect a whole region and are difficult to characterize by distinct frequencies. In contrast, single-point defects are localized and can be classified according to following affected element (M. Blodt *et al*,2008):

- Outer raceway defect.
- Inner raceway defect.
- Ball defect.

A single-point defect could be imagined as a small hole, a pit, or a missing piece of material on the corresponding element. With each type of bearing fault, a characteristics

*Corresponding author: **Habeeb J. Nekad**

frequency f_c can be associated. This frequency is equivalent to the periodicity by which an anomaly appears due to the existence of the fault.

The characteristics frequencies are functions of the bearing geometry and the mechanical rotor frequency f_r . A detailed calculation of these frequencies can be found in (B. Li *et al*,2000). For the three considered fault types, f_c takes the following expressions:

Outer raceway:

$$f_o = \frac{N_b}{2} f_r \left(1 - \frac{D_b}{D_c} \cos \beta\right) \quad (1)$$

Inner raceway:

$$f_i = \frac{N_b}{2} f_r \left(1 + \frac{D_b}{D_c} \cos \beta\right) \quad (2)$$

Ball:

$$f_b = \frac{D_c}{D_b} f_r \left(1 - \frac{D_b^2}{D_c^2} \cos^2 \beta\right) \quad (3)$$

It has been statistically shown in (R. L. Schitzl *et al*,1990) that the vibration frequencies can be approximated for most bearings with between 6 and 12 balls by:

$$\text{Outer raceway: } f_o = 0.4N_b f_r \quad (4)$$

$$\text{Inner raceway: } f_i = 0.6N_b f_r \quad (5)$$

So that, the bearing fault frequency in the stator current is given by:

$$f_{bf} = (f_1 \pm k f_c) \quad k = 1,2,3,.. \quad (6)$$

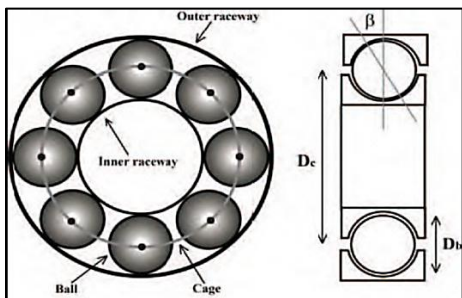


Fig.1 Structure and dimensions of bearings

3. Theoretical Study: Load Torque Variations

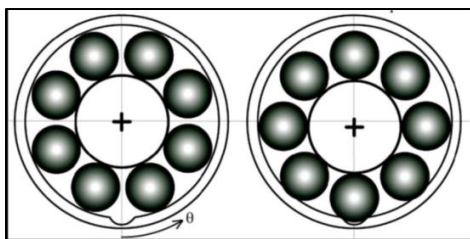


Fig. 2 Example of outer raceway defect

Imaging for example a hole in the outer raceway: each time a ball passes in a hole (as shown in Fig. (2)), a mechanical resistance will appear when the ball tries to leave the hole. The consequence is a small increase of the load torque at each contact between the defect and another bearing element.

Under a bearing fault, the load torque as a function of time can be described by a constant component T_C and an additional component varying at the characteristic frequency f_c . The first term of the variable component's Fourier series development is a cosine varying at frequency f_c . For the sake of clarity, higher order terms are neglected in the following and only the fundamental term is considered. The load torque can therefore be described by (M. Blodt *et al*,2008):

$$T_L = T_C + \Delta T = T_C + \Delta T_C \cos(\omega_c t) \quad (7)$$

$$T_e - T_L = J \frac{d\omega_r}{dt} \quad (8)$$

Bearing faults have a direct impact on the torque of the machine and cause load torque oscillations. The effect of load torque oscillations on the q-component of the stator current has been studied in this paper.

4. Discrete Wavelet Transform (DWT)

DWT actually splits a signal to several band-limited signals, the sum of which is equal to the original one. In this way, the original signal can be reconstructed as a sum of n detail signals ($D_j, 1 \leq j \leq n$) and an approximation signal (A_n). Each detail D_j includes frequency components $[2^{-(j+1)} \cdot f_s, 2^{-j} \cdot f_s]$, while the approximation signal includes all the lower frequency components, including the dominant DC signal. More specifically, at each level of DWT decomposition, low-pass ($g[n]$) and high-pass ($h[n]$) filters are applied (I. Georgakopoulos *et al*,2010).

5. Neural Network Structure

The artificial neural networks are highly connected network of elementary processors running in parallel. Each elementary processor computes a single output based on information it receives. Two main elements constitute an artificial neural network: the neuron model used to build the network and then the network architecture. Each artificial neuron is an elementary processor that receives a number of neural inputs upstream (Z. M. Taibi *et al*,2011).

In ANN, two layers of neuron communicate via a weight connection network. The type of weighted connections used in this network is the feed-forward neural network, which composed by: (an input layer, one or more hidden layers, and an output layer). The mathematical model of neuron is presented by:

$$y = f(\sum_{i=1}^n w_i x_i - b) \quad (9)$$

In this work, the structure of the neural network consists of an input layer that is fed by seven inputs (the RMS values of the wavelet coefficients ($A_6, D_6, D_5, D_4, D_3, D_2,$ and D_1)), an output layer and two hidden layers. The RMS value of the discrete signal S can be determined by

$$S_{RMS} = \sqrt{\left(\frac{1}{N} \sum_{i=1}^N s_i^2\right)} \quad (10)$$

The neural network model is trained by using Levenberg-

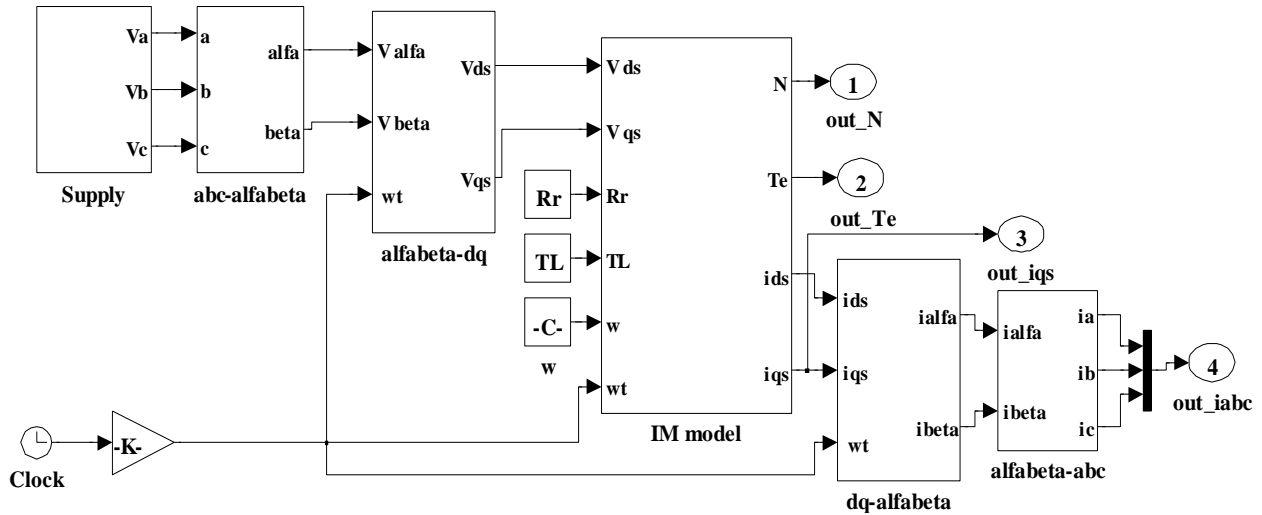


Fig. 3 Induction motor simulation model

Marquardt algorithm. The network has two outputs (1 for healthy motor and 0 for bearing fault).

6. Proposed Method

For study the bearing faults, a simulation model for the three-phase induction motor has been derived based on the mathematical model in a synchronously rotating reference frame using matlab/simulink. The simulink model implemented in this paper is shown in Fig.(3). It consists of conversion blocks and motor dq-model as follows:-

A. abc-dq conversion

To convert 3-phase voltage to voltages in the 2-phase synchronously rotating frame, they are first converted to 2-phase stationary frame (α, β) and then from the stationary frame to the synchronously (dq) rotating frame. The transformation is given by the following equations [9,10]:

$$\begin{bmatrix} v_\alpha \\ v_\beta \end{bmatrix} = \sqrt{\frac{2}{3}} \begin{bmatrix} 1 & -\frac{1}{2} & -\frac{1}{2} \\ 0 & \frac{\sqrt{3}}{2} & -\frac{\sqrt{3}}{2} \end{bmatrix} \begin{bmatrix} v_a \\ v_b \\ v_c \end{bmatrix} \tag{11}$$

$$\begin{bmatrix} v_d \\ v_q \end{bmatrix} = \begin{bmatrix} \cos\theta & \sin\theta \\ -\sin\theta & \cos\theta \end{bmatrix} \begin{bmatrix} v_\alpha \\ v_\beta \end{bmatrix} \tag{12}$$

B. Motor dq-Model

The dq-model of induction motor is represented according to the following equations:

$$v_s^{dq} = R_s i_s^{dq} + \frac{d\lambda_s^{dq}}{dt} + \omega \begin{bmatrix} 0 & -1 \\ 1 & 0 \end{bmatrix} \lambda_s^{dq} \tag{13}$$

$$0 = R_r i_r^{dq} + \frac{d\lambda_r^{dq}}{dt} + (\omega - \omega_r) \begin{bmatrix} 0 & -1 \\ 1 & 0 \end{bmatrix} \lambda_r^{dq} \tag{14}$$

$$\lambda_s^{dq} = (L_f + L_m) i_s^{dq} + L_m i_r^{dq} \tag{15}$$

$$\lambda_r^{dq} = L_m i_s^{dq} + L_m i_r^{dq} \tag{16}$$

$$T_e = \frac{3P}{2} L_m (i_{qs} i_{dr} - i_{ds} i_{qr}) \tag{17}$$

C. dq-abc Conversion

This conversion does the opposite of the abc-dq conversion for the current variables.

In the present work, DWT uses q-axis current (i_{qs}) so as to identify bearing fault. Daubechies-44 wavelet (db44) has been used as a mother wavelet. The supply frequency in this paper is taken to be 50 Hz and table I shows the frequency level of the wavelet coefficients.

Table 1 Frequency level of the wavelet coefficients.

Level	Frequency Band with $f_s=5000$ samples/sec
D1	1250-2500 Hz
D2	625-1250 Hz
D3	312.5-625 Hz
D4	156.25-312.5 Hz
D5	78.12-156.25 Hz
D6	39.06-78.12 Hz
A6	0-39.06 Hz

7. Simulation Results

The motor used in the simulation study is 1.1 KW, 220V, 50Hz (see appendix), 2-pole induction motor. Fig. (4) shows the wavelet coefficients of (i_{qs}) for healthy motor under transient conditions with full load ($T_C = 5N.m$). Also, Fig. (5) shows the wavelet coefficients of (i_{qs}) for bearing fault (outer raceway) case (with additional component of load torque $\Delta T_C = 0.2T_C$). Speed, developed electromagnetic torque, and stator q-axis current component of induction motor for different cases are shown in Figs. (6-8), respectively.

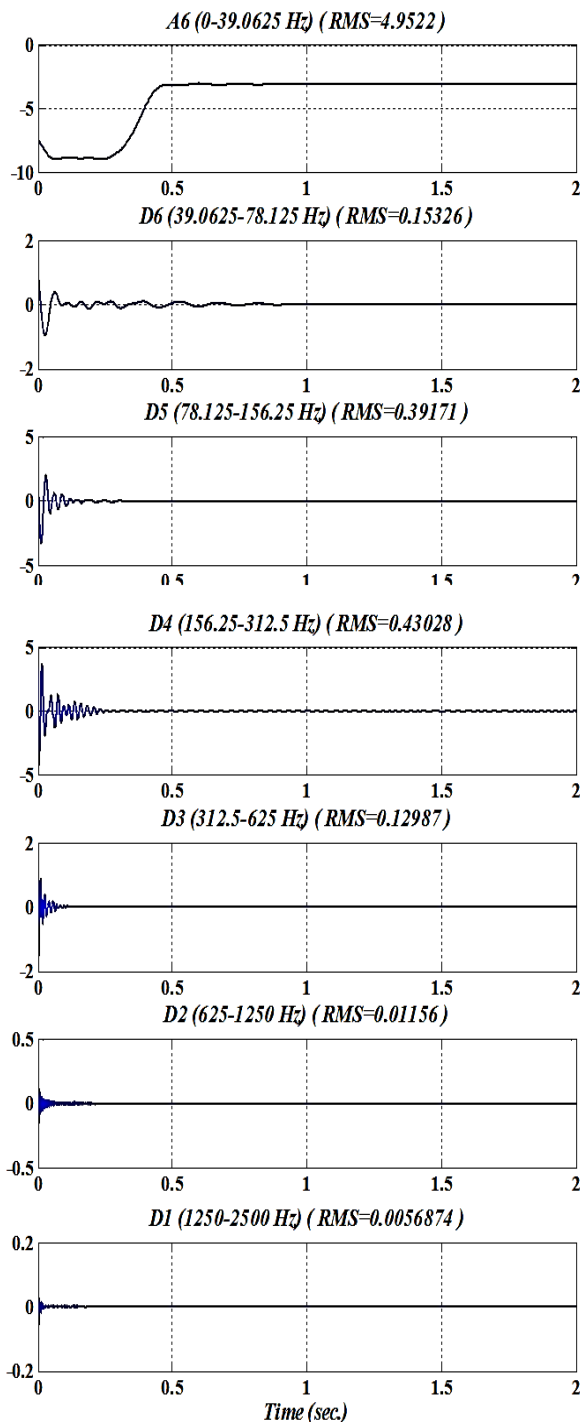


Fig.4 Wavelet coefficients of stator q-axis current component for healthy machine with full load

The RMS values of the wavelet coefficients for level 6 are then be used as the inputs of the neural network to give an output which identifies the machine case. Training data of all the input parameters (wavelet coefficients) are applied for obtaining the optimized architecture for the detection of bearing fault of an induction motor as shown in Fig. (9). The input data set are composed by a successive range of several examples in different operating conditions of the induction motor (no load , 5% load, 10% load,..., full load). In Fig. (9), the input data represent different

operating cases of the induction motor: healthy (20 points) and bearing fault (40 points for outer and inner raceway faults). Thus, a total of 60 training points have been collected and useful for studying bearing faults.

Figs. (10) and (11) show the ANN output and error for healthy and bearing fault of an induction motor respectively. Fig. (10) describes that the output of the ANN from which the star one is the target value (either 0 or 1 for healthy and bearing fault condition respectively) and the circle one is the actual output of the ANN.

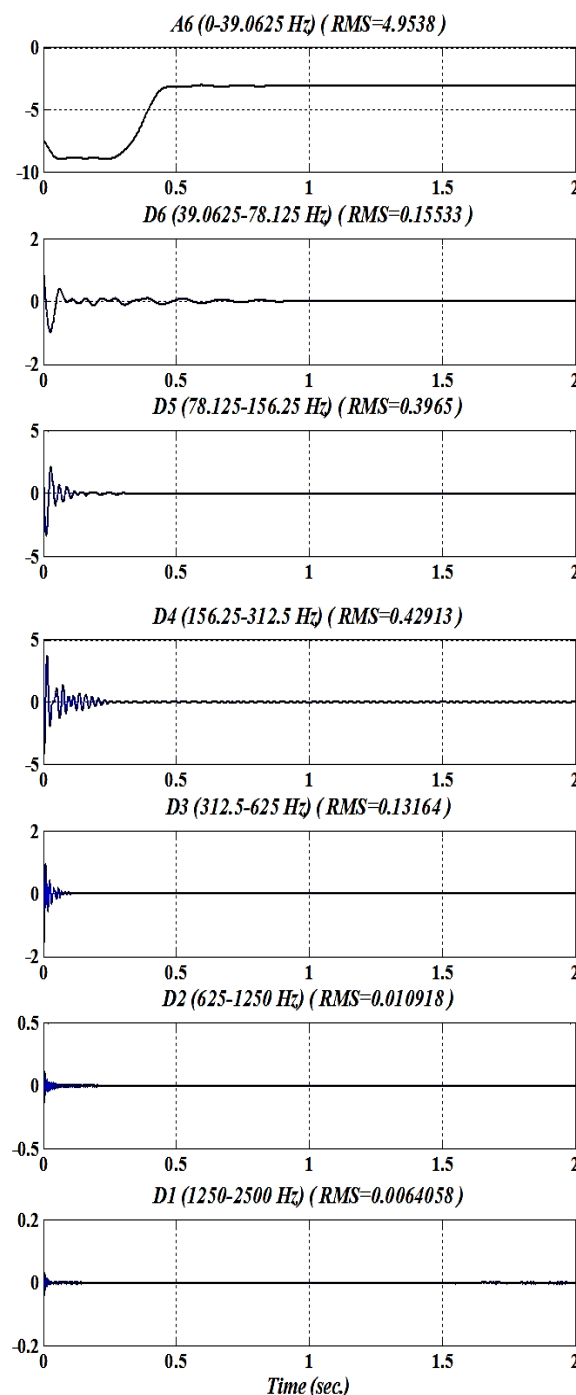


Fig.5 Wavelet coefficients of stator q-axis current component for outer raceway bearing fault ($\Delta T_c = 0.2T_c$) at full load

From Fig. (10) it is clear that the ANN has well learned the input data and correctly produced the desired output. Hence, the error which is the difference between the target value and the actual output value is 1×10^{-8} which is shown in Fig. (11).

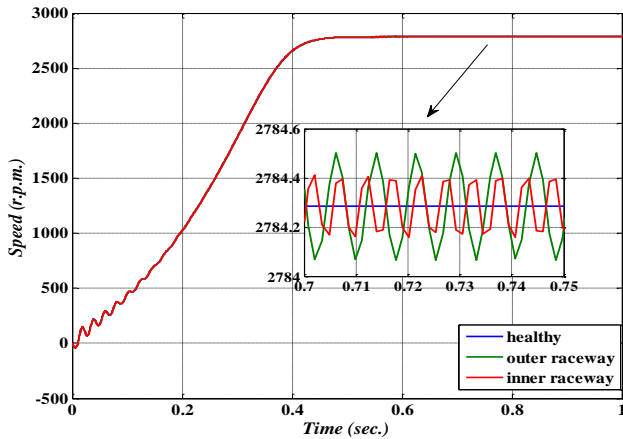


Fig. 6 Speed of 3-ph I.M. for different types of bearing faults at full load

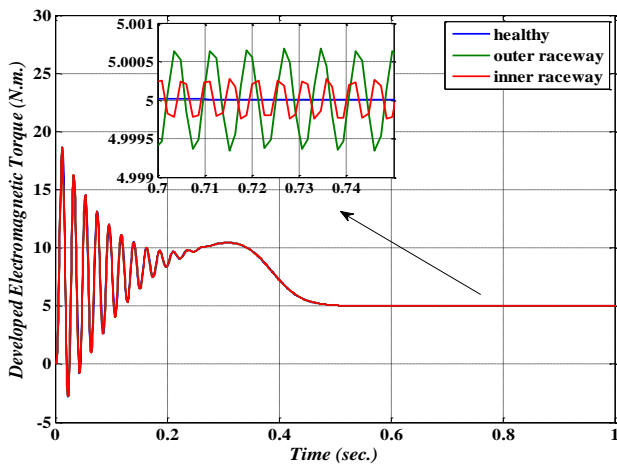


Fig 7 Developed electromagnetic torque of 3-ph I.M. for different types of bearing faults at full load

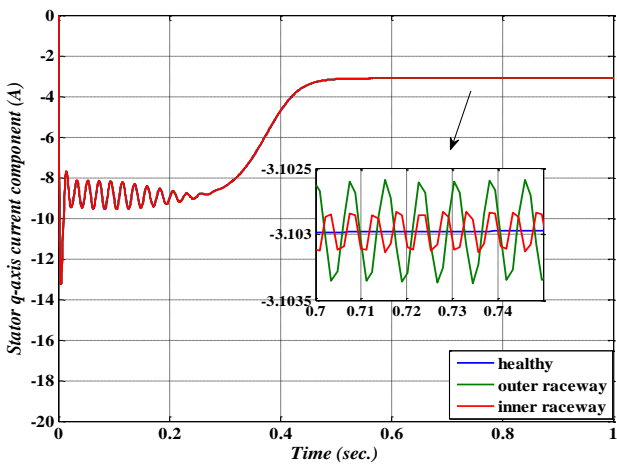


Fig.8 Stator q-axis current component of 3-ph I.M. for different types of bearing faults at full load

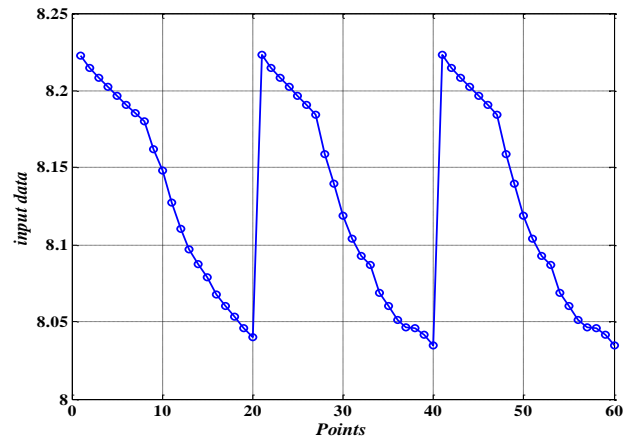


Fig.9 Training data of induction motor (A6 RMS values) with bearings fault

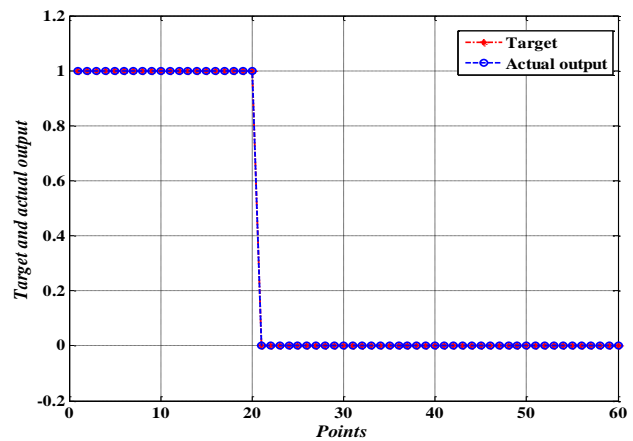


Fig.10 ANN output with bearing faults

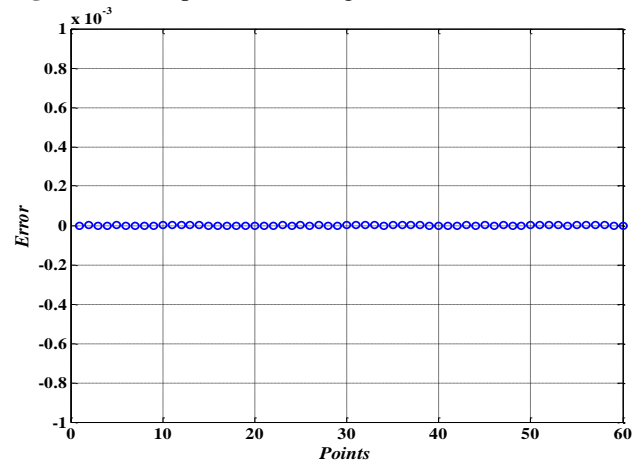


Fig.11 ANN error with bearing faults

Conclusion

This paper presents an effective method for bearing fault diagnosis of induction motor under transient conditions. Where, we carried out induction motor fault detection using DWT of the q-axis component of the stator current. Simulation results are developed by ANN which gives better identification of the motor state.

The good simulated results show that the proposed method allows an accurate diagnosis of the bearing fault

under different load and transient conditions. Future works are focus on different conditions for different faults of induction motor.

Appendix

Motor Parameters:

P_n : 1.1KW, V_s : 220V, f_1 : 50Hz

P : 1, R_s : 7.58 Ω , R_r : 6.3 Ω

L_f : 26.5mH, L_m : 46.42mH

J : 0.0054 kg m²

Nomenclature

D_b ball diameter

D_c cage diameter

f_i supply frequency

f_c characteristics frequency

f_r mechanical rotor frequency

f_s sampling frequency

i_{ds}, v_{ds} stator d-axis current and voltage

i_{dr}, v_{dr} rotor d-axis current and voltage

i_{qs}, v_{qs} stator q-axis current and voltage

i_{qr}, v_{qr} rotor q-axis current and voltage

J inertia of motor

L_f leakage inductance

L_m mutual inductance

N_b number of balls

P pole number

R_s stator phase resistance

R_r rotor phase resistance

S discrete signal

T_C constant torque

T_e electrical torque

T_L load torque

ϕ_s stator flux

ϕ_r rotor flux

θ transformation angle

β contact angle

References

- W. Saadaui and K. Jelassi (2011), Induction Motor Bearing Damage Detection Using Stator Current Analysis, Proceedings of the 2011 *International Conference on Power Engineering, Energy and Electrical Drives*.
- L. Frosini and E. Bassi (2010), Stator Current and Motor Efficiency as Indicators for Different Types of Bearing Faults in Induction Motor, *IEEE Transactions on Industrial Electronics*, Vol. 57, No.1
- M. E. Benbouzid (2000), A Review of Induction Motors Signature Analysis as a Medium for Faults Detection, *IEEE Transactions on Industrial Electronics*, Vol. 47, No. 5, pp. 984-993.
- M. Blodt, P. Granjon, B. Raison, and G. Rostaing (2008), Models for Bearing Damage Detection in Induction Motors Using Stator Current Monitoring, *IEEE transactions on Industrial Electronics*, Vol. 55, No. 4, pp. 1813-1822.
- B. Li, M. Chow, Y. Tipsuwan, and J. Hung (2000), Neural-Network-Based Motor Rolling Bearing Fault Diagnosis, *IEEE Transactions on Industrial Electronics*, Vol. 47, No. 5, pp. 1060-1069.
- R. L. Schitzl (1990), Forcing Frequency Identification of Rolling Element Bearings, *Sound Vibrations*, Vol. 24, No. 5, pp. 16-19.
- I. Georgakopoulos, E. Mitronikas, A. Safacas (2010), Broken Bar Detection Using Inverter Currents in Induction Motor Drives, *SPEEDAM*, pp. 1030-1035.
- Z. M. Taïbi, M. Hasni, S. Hamadani, O. Rahmani, O. Touhami, and R. Ibtouen (2011), Optimization of the Feed forward Neural Network for Rotor Cage Fault Diagnosis in Three-Phase Induction Motor, *IEEE International Electric Machines and Drives Conference (IEMDC)*, pp. 194-199.
- J. Lee, P. Pillay, and R. G. Harley (1985), D,Q Reference Frames for the Simulation of Induction Motors, Department of Electrical Engineering, University of Natal, *Electric Power Systems Research, Regular Papers*, 8
- B. A. Kumari, K. N. Sujatha, K. Vaisakh (2009), Dept. of Electrical Engineering, Assessment of Stresses on Induction Motor Under Different Fault Conditions, *Journal of Theoretical and Applied Information Technology*, Vol. 50, 2009.